Atmospheric Environment 69 (2013) 65–75

Contents lists available at SciVerse ScienceDirect

Atmospheric Environment

journal homepage: www.elsevier.com/locate/atmosenv

Ultrafine particle concentrations in and around idling school buses

Qunfang Zhang [a], Heidi J. Fischer [b], Robert E. Weiss [b], Yifang Zhu [a,*]

[a] Department of Environmental Health Sciences, UCLA Fielding School of Public Health, Los Angeles, CA 90095-1772, USA
[b] Department of Biostatistics, UCLA Fielding School of Public Health, Los Angeles, CA 90095-1772, USA

HIGHLIGHTS

- Five scenarios were simulated to assess their impacts on UFP levels in and around idling school bus.
- Idling increased total particle number concentration near the school buses under all scenarios.
- The impact of idling on in-cabin UFP number concentrations depended on wind direction and window position.
- The deposition rates inside school cabins were lower than those of passenger cars but higher than those of indoor environments.

ARTICLE INFO

Article history:
Received 23 August 2012
Received in revised form
3 December 2012
Accepted 4 December 2012

Keywords:
Ultrafine particles
$PM_{2.5}$
School bus
Wind direction
Window position
Deposition rate

ABSTRACT

Unnecessary school bus idling increases children's exposure to diesel exhaust, but to what extent children are exposed to ultrafine particles (UFPs, diameter < 100 nm) in and around idling school buses remains unclear. This study employed nine school buses and simulated five scenarios by varying emissions source, wind direction, and window position. The purpose was to investigate the impact of idling on UFP number concentration and $PM_{2.5}$ mass concentration inside and near school buses. Near the school buses, total particle number concentration increased sharply from engine off to engine on under all scenarios, by a factor of up to 26. The impact of idling on UFP number concentration inside the school buses depended on wind direction and window position: wind direction was important and statistically significant while the effect of window positions depended on wind direction. Under certain scenarios, idling increased in-cabin total particle number concentrations by a factor of up to 5.8, with the significant increase occurring in the size range of 10–30 nm. No significant change of in-cabin $PM_{2.5}$ mass concentration was observed due to idling, regardless of wind direction and window position, indicating that $PM_{2.5}$ is not a good indicator for primary diesel exhaust particle exposure. The deposition rates based on total particle number concentration inside school bus cabins varied between 1.5 and 5.0 h^{-1} across nine tested buses under natural convection conditions, lower than those of passenger cars but higher than those of indoor environments.

1. Introduction

Diesel exhaust has been classified as a potential carcinogen by the United States Environmental Protection Agency (U.S.EPA, 2002). On a number basis, particles emitted by diesel engines are primarily in the ultrafine particle (UFP, diameter < 100 nm) size range, which have been suggested to be more toxic to laboratory animals and humans than fine and coarse particles per unit mass of particles (Alessandrini et al., 2006; Delfino et al., 2005; Ferin et al., 1990; Frampton et al., 2006). Because of their small size and large surface area, UFPs can evade alveolar macrophage clearance from the lung, penetrate the epithelium, enter the circulatory system, and deposit in the brain (Oberdorster et al., 2004; Samet et al., 2009). Children are more sensitive to UFPs because their physiological and immunological systems are still developing. Compared with adults, they receive a higher dose of particulate matter (PM) to their lung due to a greater fractional deposition with each breath and larger ventilation rate relative to lung size (Bennett and Zeman, 1998).

In the U.S., there are about 25 million children riding school buses daily, about 90% of which are powered by diesel (U.S.EPA, 2012). The concentrations of vehicle emitted air pollutants, such as UFPs, black carbon (BC), particle-bound polycyclic aromatic hydrocarbon, and NO_2, were higher inside conventional diesel-powered school buses than inside clean natural gas school buses or at nearby background sites (Behrentz et al., 2005; Sabin et al., 2005; Zhang and Zhu, 2010). Even though school bus commutes

* Corresponding author. Tel.: +1 310 825 4324; fax: +1 310 794 2106.
E-mail addresses: zhangqunfang@gmail.com (Q. Zhang), heidi.j.fischer@gmail.com (H.J. Fischer), robweiss@ucla.edu (R.E. Weiss), Yifang@ucla.edu (Y. Zhu).

1352-2310/$ – see front matter © 2012 Elsevier Ltd. All rights reserved.
http://dx.doi.org/10.1016/j.atmosenv.2012.12.015

accounted for less than 10% of a child's day, they contributed 33% of a child's daily exposure to BC (Behrentz et al., 2005). The emission-to-individual intake ratio of school bus emissions per on-board student was estimated to be 10^5–10^6 times greater than for a typical resident in the South Coast Air Basin (Marshall and Behrentz, 2005).

To protect children from diesel exhaust emitted by school buses, the U.S. EPA launched a series of programs, including retrofitting old diesel-powered school buses with certified retrofit technologies, promoting the use of cleaner fuel, and eliminating unnecessary idling. The use of retrofit devices and alternative cleaner fuel were found to lower particle emissions from engine combustion process (Jayaratne et al., 2009; Zhang and Zhu, 2011). However, the impact of anti-idling practices to reduce children's exposure to UFPs remains unclear.

Diesel emissions from idling school buses could reach children through different routes. First, diesel emissions from one school bus could penetrate into its own cabins through cracks, doors, and windows. This so-called "self-pollution" increases the exposure of children on board, and has been quantified by the tracer gas method. Using SF_6 as a tracer, Behrentz et al. (2004) estimated that up to 0.3% of in-cabin air came from a bus's own exhaust. Using iridium as a fuel-based tracer, self-pollution was estimated to contribute 0.1%–41% of in-cabin $PM_{2.5}$ (Ireson et al., 2004, 2011; Liu et al., 2010). Diesel emissions can also enter the cabins of nearby school buses. High in-cabin air pollutant levels were observed at the bus transfer station and the school parking lot where many school buses were idling simultaneously (Zhang and Zhu, 2010). In addition, idling school buses can increase air pollutant concentrations in vicinity of the buses while many school children are waiting to board. The presence of school buses was linked with a consistent increase in the total particle number concentration during drop-off/pick-up hours (Hochstetler et al., 2010), and the number of idling buses and trucks was positively associated with black carbon levels on the street canyon near a cluster of schools (Richmond-Bryant et al., 2011, 2009). Few studies, however, have been conducted to systematically assess the impact of idling on air pollutant concentrations in and around school buses. This study investigated the impact of idling on UFP number concentration and $PM_{2.5}$ mass concentration inside and near school buses by simulating five scenarios of different emission sources, wind directions, and window positions. The results facilitate the assessment of anti-idling practices in reducing children's exposure to UFPs.

After penetrating into bus cabins, particles are removed by several mechanisms, including air exchange with outdoor air, inhalation and deposition. As an important particle removal mechanism, UFP deposition rate is critical to estimate UFP exposure inside school buses. Although in-cabin particle deposition has been studied inside passenger vehicles (Gong et al., 2009; Ott et al., 2008), those results may not be applicable to school buses owing to the uniqueness of in-cabin geometric structures and surface area to volume ratios of school buses. To fill in this knowledge gap, this study also measured the UFP deposition rates in nine school buses.

2. Methods

2.1. School buses and sampling site

This study was conducted in an open space without nearby UFP emission source about 5 miles from the coast line in Los Angeles, CA. During the study period, daily wind direction and wind speed ranged from 179 to 205°and from 2.5 to 3.6 m s^{-1}, respectively. Temperature and relative humidity varied from 18 to 22 C° and from 62 to 78% respectively. The stable meteorological condition reduced day-to-day variability of background pollutant concentrations leading to a better signal to noise ratio. Nine school buses from a local transportation company serving the greater Los Angeles area were employed between August 3 and September 10, 2010. The characteristics of tested school buses are shown in Table S1 in the supporting information (SI). One bus was model year 1999 and the other eight were model year 2005. There was no AC/fan unit in these buses. All bus engines were located in the front hood. No emission control was applied to these school buses at the time of testing.

2.2. Scenario simulation

Five scenarios were simulated by varying emission source, wind direction, and window position. The layout of school buses for each scenario are shown in a simple sketch in Fig. 1. Arrows indicate wind directions; boxes represent bus bodies; and gray areas indicate the emission sources from idling school buses. Constant wind direction during the study period allowed positioning of the buses either parallel to the wind, so that the bus cabin was downwind of the tailpipe emissions, or perpendicular to the wind, where the cabin was upwind of the tailpipe emissions. Diesel emissions were either from the tested school buses' own tailpipes or from the tailpipe of the nearby school bus. Two window positions were tested for each simulated scenario: (1) all windows were closed, although some of the windows could not be closed tightly; or (2) eight rear windows, four on each side, were opened 20 cm.

Scenarios 1 and 2 used one school bus. In scenario 1 (Fig. 1(a)), each school bus was parked perpendicular to wind direction. Air quality data were collected alternatively with the engine off and on for approximately 30 min each. In scenario 2 (Fig. 1(b)), the bus was rotated 90° to simulate a parallel wind, so that the wind blew from the bus' tailpipe toward its hood. Scenarios 3–5 employed two school buses parked at 90° degrees to each other with the tailpipe of one pointing to the side of the other near the back at a distance of about 2 m between their tailpipes. The upwind bus was perpendicular to the wind and the other bus was parallel to the wind along the downwind side. Air quality data were first collected with both bus engines off for 30 min. In scenario 3 (Fig. 1(c)), only the engine of the downwind bus was turned on for 30 min. Air quality data in and around the upwind bus were collected. In scenario 4 (Fig. 1(d)), only the engine of the upwind bus was turned on and the air quality data in and around the downwind bus were collected for 30 min. In scenario 5 (Fig. 1(e)) the engines of both buses were turned on, and air quality data in and around both buses were collected for 30 min.

Doors remained closed and the bus was unoccupied during the measurements. Other than the buses being tested, no school buses were allowed to operate nearby. In the absence of emission sources on the upwind side, the difference of air pollutant concentrations between engine off and engine on conditions was primarily attributed to emissions from the idling buses. Scenarios 1 and 2 investigated the contribution of self-pollution with a perpendicular and parallel wind, respectively. Scenarios 3 and 4 investigated the impact of the emissions from idling buses on nearby buses. Scenario 5 investigated the worst scenario with more than one bus idling close together such as at a bus transfer station or school parking lot.

2.3. Measurement of air exchange rate and deposition rate

For each school bus, air exchange rates were estimated by the CO_2 decay method (Zhu et al., 2005). From a compressed CO_2 cylinder, CO_2 was released into the cabin until the concentration was higher than 2000 ppm. The decay of CO_2 concentration was measured by a TSI Q-trak indoor air quality monitor (Model 8550, TSI Inc., St. Paul, MN). The air exchange rate was calculated by

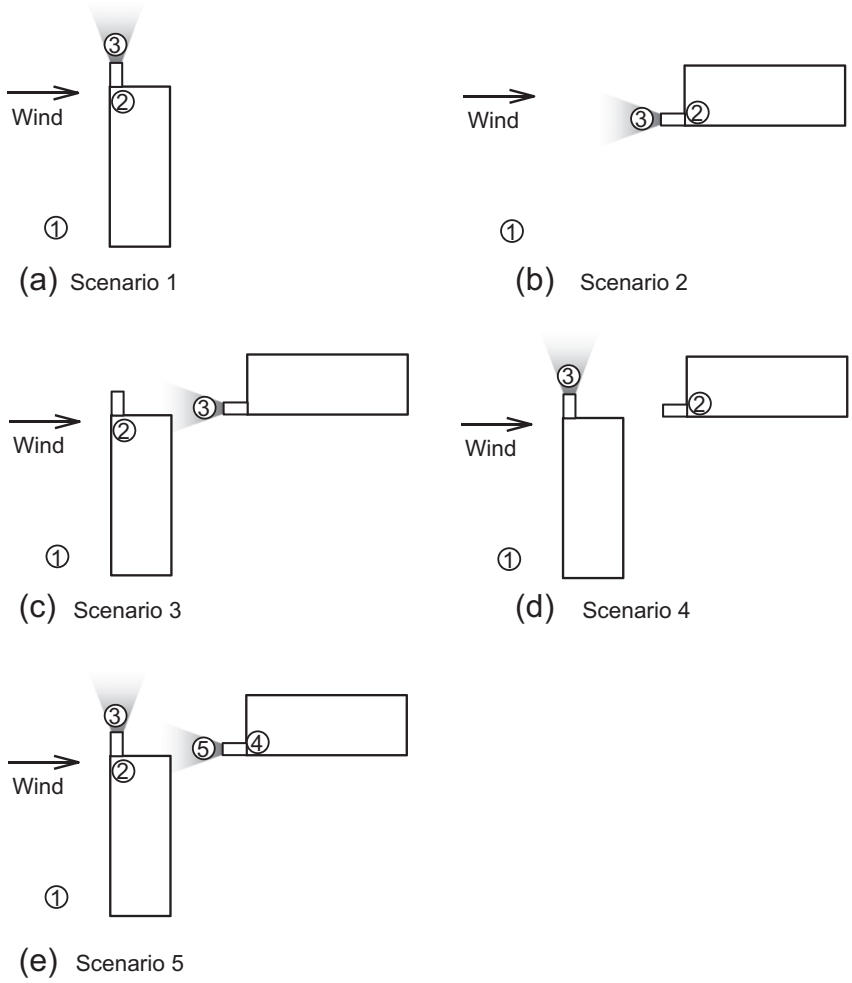

Fig. 1. Schematic layout of tested school buses and instruments for different scenarios. Open boxes are school bus bodies, gray areas indicate tailpipe emissions, and open circles with numbers are locations of the air pollutant measuring equipment.

$$\lambda = \frac{1}{t - t_0} \ln\left(\frac{C_{in}(t) - \overline{C_{out}}}{C_{in}(t_0) - \overline{C_{out}}}\right) \quad (1)$$

where λ is the air exchange rate (h^{-1}); t_0 and t are the beginning and end of the sampling interval (h); the averaged outdoor CO_2 concentrations (ppm) for the period from t_0 to t is $\overline{C}_{out}$; the indoor CO_2 concentrations (ppm) measured at time t and t_0 are $C_{in}(t)$ and $C_{in}(t_0)$, respectively (Zhu et al., 2005).

Particle deposition rates were determined for each bus. Each tested school bus was parked parallel with the wind direction and with 8 rear windows open by 20 cm. The engine was turned on so that diesel particles emitted by the tailpipes were carried by the wind and entered the cabin through open windows as the particle sources for deposition. After about 15 min, the engine was turned off and all the windows and doors were closed. The decay of in-cabin particle number concentration was recorded by a scanning mobility particle sizer (SMPS; Model 3936L85, TSI Inc., St. Paul, MN) placed on the rear seat. Each test lasted for about 20–30 min until the in-cabin UFP concentrations approached ambient levels and it was repeated 2–3 times for each bus. Deposition rate was calculated as

$$\ln\left(\frac{PNC(t)}{PNC(0)}\right) = -(\lambda + k)t \quad (2)$$

(Gong et al., 2009) where PNC(t) and PNC(0) are the particle number concentrations (particles/cm^3) measured at time t and 0, respectively. The air exchange rate (h^{-1}) and the deposition rate (h^{-1}) are indicated by λ and k, respectively. Deposition rates were calculated for particles of each size to estimate size-resolved UFP deposition rates. The sum over all sizes of the particle concentrations were used to calculate the deposition rate for total particles. The in-cabin volume and the interior surface area were determined for each bus. Interior surface materials were the same for all buses, including rubber, plastic, artificial leather, metal, and glass. Additional areas of in-cabin geometric structure such as seats, dashboards and the equipment were included as interior surface areas.

2.4. Instruments

For each scenario, air quality of the upwind air, in-cabin air, and air close to the tailpipes were measured simultaneously, as summarized in Table 1. For the upwind air, a condensation particle counter (CPC; Model 3781, TSI Inc., St. Paul, MN) and a TSI DustTrak photometer (Model 8520 TSI, Inc., St. Paul, MN) with a $PM_{2.5}$ inlet impactor measured total particle number concentration and $PM_{2.5}$ mass concentration at 1 m height and 2 m upwind of the tested bus, respectively. For the air close to the tailpipes, a CPC (Model 3007 TSI, Inc., St. Paul, MN) measured

Table 1
Instruments and measured parameters.

Species	Instrument		
	Upwind	Tailpipe	In-cabin
Total particle number	TSI CPC[a] 3781	TSI CPC 3007	TSI SMPS[b,c]
Particle size distribution			TSI SMPS
$PM_{2.5}$	TSI DustTrak 8520		TSI DustTrak 8520
CO_2	TSI Q-trak 7565		TSI Q-trak 7565

[a] Condensation particle counter.
[b] Scanning mobility particle sizer.
[c] The number concentrations of particles with diameter between 7.6 and 289 nm measured by the SMPS was summed up as total particle number concentration for the in-cabin air.

total particle number concentration at the height of tailpipes and 0.5 m away from the point of the tailpipe exhaust. For in-cabin air quality, a SMPS, a DustTrak, and a Q-trak were placed on the rear seat of the buses to measure particle size distribution, $PM_{2.5}$ mass concentration, and CO_2, respectively. The number concentrations of particles with diameters between 7.6 and 289 nm measured by the SMPS were summed to calculate the in-cabin air total particle number concentration. For scenario 5, since the air quality of both the upwind and the downwind buses were measured simultaneously, two identical sets of instruments were used simultaneously. The identical instruments were collocated to collect data side by side for at least 10 min before and after each test to determine the relationship of their readings. A detailed description of instruments can be found in the SI.

2.5. Statistical analysis

We modeled the effect of engine operation on in-cabin particle levels over time under different scenarios using longitudinal regression analysis (Weiss, 2005). In-cabin particle number concentrations for each particle size, total particle number concentration, and $PM_{2.5}$ mass concentration were analyzed using separate longitudinal regressions. Longitudinal models were fit with the SAS mixed procedure (SAS Version 9.2; SAS Institute, Cary, NC, USA).

All outcomes were analyzed after log transformation to stabilize variance and linearize the relationship with time. We used a first-order autoregressive moving average model (ARMA) to account for the correlation of observations on a single bus over time which fit best over the many correlation models considered. With the engine off, we assumed that the in-cabin UFPs were constant across different scenarios, though different for different size particles. With the engine on, the UFP number concentrations were modeled as linear with time with slopes differing by scenario. Data collected under scenarios 1–4 were used to estimate the effects of window position (closed/open), wind direction (parallel/perpendicular), emission source (buses' own tailpipe or other buses' emissions), and all two-way interactions on log in-cabin particle number concentrations for each particle size. The mean of exp (X) where X is a normal random variable with mean μ and variance σ^2 is $M = \exp(\mu + 0.5\sigma^2)$. When μ and σ^2 are estimated by $\hat{\mu}$ and $\hat{\sigma}^2$, we can estimate the particle count on the unlogged scale as $\hat{M} = \exp(\hat{\mu}+0.5\hat{\sigma}^2)$, though this may underestimate the count due to ignoring uncertainty in $\hat{\mu}$and$\hat{\sigma}^2$. We get$\hat{\mu}$, $\hat{\sigma}^2$and their standard errors from the SAS proc mixed output where $\hat{\mu}$ represents any mean estimate on the logged scale. To get a 95% CI for $\hat{M}$, we simulate $\hat{M}_k = \exp(\hat{\mu}_k + 0.5\hat{\sigma}_k)$, where $\hat{\mu}_k$and $\hat{\sigma}_k$ are generated from independent normal distributions with means $\hat{\mu}$ and $\hat{\sigma}^2$, and standard errors SE($\hat{\mu}$) and SE($\hat{\sigma}^2$), respectively. If $\hat{\sigma}_k$ is negative, we set it equal to 0. We repeat for $k = 1, \ldots, K$; we took $K = 1000$. This assumes that the estimates of μ and σ^2 are independent and normal, which indeed they are asymptotically. We estimate M by the mean of the M_k's and construct a 95% CI by taking the 2.5% and 97.5% quantiles of the M_k's.

3. Results and discussion

3.1. Ultrafine particles in and around school buses

Fig. 2 summarizes the average total particle number concentrations under engine off and engine on conditions for the upwind air, the in-cabin air, and the air close to tailpipes under different scenarios. For each bus and scenario, average concentrations were calculated under engine off and engine on conditions. The mean and standard deviation of these nine average concentrations were calculated to present the overall change of particle levels due to engine operation in Fig. 2. Detailed time series of total particle number concentration under engine off and engine on conditions are shown in Figure S1-S3 in the SI.

Indicated by the small variation of average total particle number concentration in the upwind air, the background particle levels were fairly stable, varying between from 8.2×10^3 to 10.9×10^3 particles/cm^3. For the air close to tailpipes, average total particle number concentrations were about the same level as the background with engine off. After turning on the engines, particle levels close to tailpipes increased sharply to 112.0×10^3 to 315.7×10^3 particles/cm^3. Such a sharp increase indicates potentially high exposure to diesel particles for children waiting to board near idling school buses.

The change in average in-cabin total particle number concentrations depended on wind direction and window position. In Fig. 2(a), with perpendicular wind, no distinct change was measured after turning on the engines, regardless of window positions. With parallel wind in Fig. 2(b), the average in-cabin total particle number concentrations increased from 11.1×10^3 to 16.0×10^3 particles/cm^3 with closed windows ($p = 0.07$) and increased from 8.3×10^3 to 23.4×10^3 particles/cm^3 with open windows ($p < 0.001$). The penetration of tailpipe emissions from other buses idling nearby depended on bus position. In Fig. 2(c), the change in in-cabin total particle number concentrations in the upwind bus due to engine operation of the downwind bus was negligible. The penetration of tailpipe emissions from upwind bus to the downwind bus cabins was more evident. In Fig. 2(d), after turning on the upwind bus' engine, the average in-cabin total particle number concentrations increased from 11.5×10^3 to 14.0×10^3 particles/cm^3 with closed windows ($p = 0.14$) and from 7.3×10^3 to 21.3×10^3 particles/cm^3 with open windows ($p = 0.02$). When two school buses were idling together as in Fig. 2(e), after turning on the engines, no increase of in-cabin total particle number concentrations was measured in the upwind bus regardless of window positions, nor in the downwind bus when the windows were closed as in Fig. 2(f). However, when the windows were open, the downwind bus had the greatest increase of average in-cabin total particle number concentration, going from 7.6×10^3 for engine off condition to 36.8×10^3 particles/cm^3 for engine on condition ($p < 0.001$).

The ratio of average total particle number concentrations between engine on and engine off conditions for the different scenarios are summarized in Fig. 3. Ratios for upwind air ranged from 1.0 to 1.1, indicating that the upwind air was not affected by tailpipe emissions. The tailpipe air ratios were the highest, with a maximum of 26.0. Ratios for the in-cabin air varied with wind direction and window position. For closed windows the ratios were

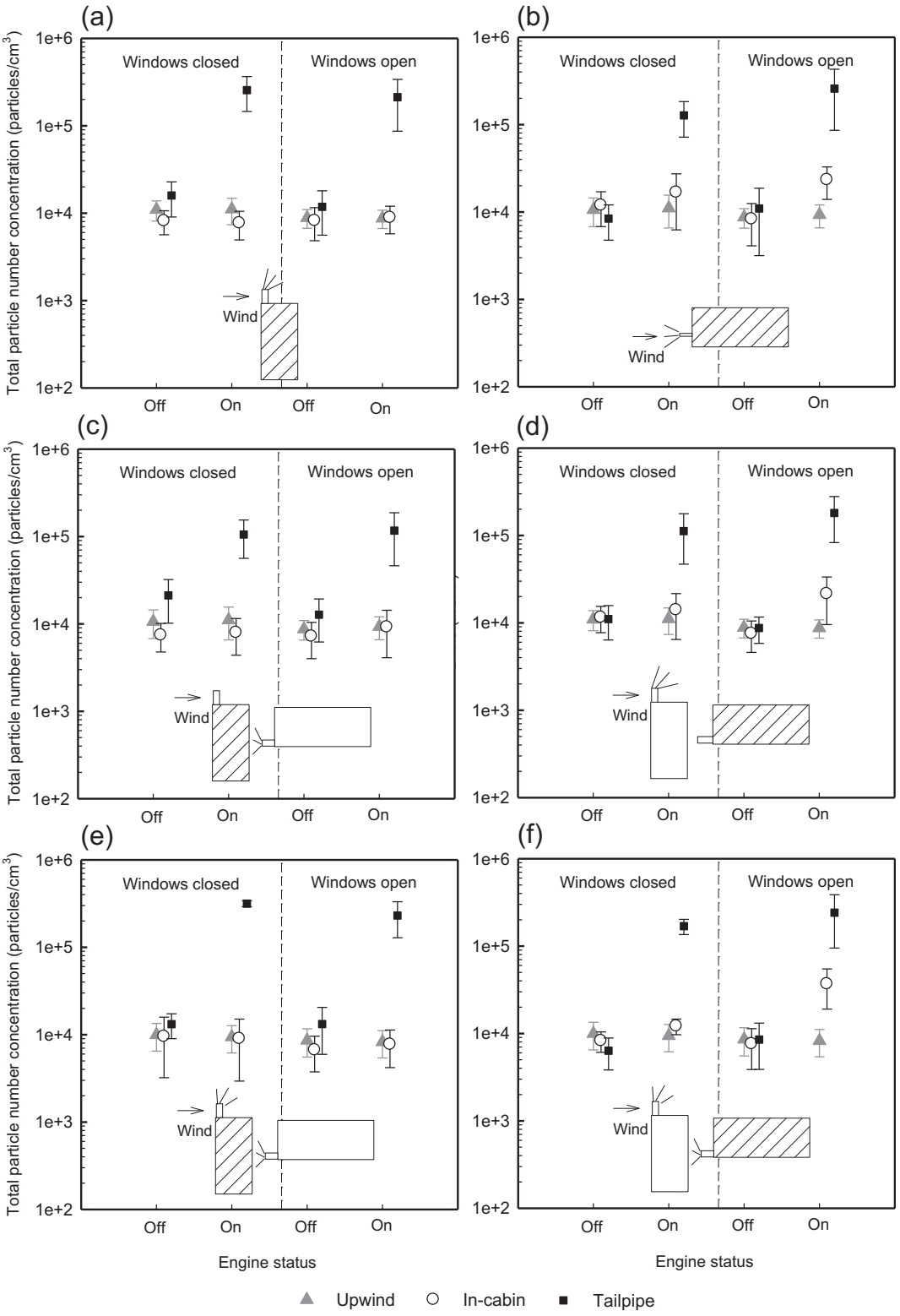

Fig. 2. Total particle number concentrations for upwind air, in-cabin air, and air close to tailpipes under different scenarios with different window positions. Shaded boxes indicate the buses in which the measurements come from. Rays indicate the buses for which the engines were turned on. Error bars indicate one sample standard deviation. Figures (a) – (d) present scenarios 1 – 4 and (e) – (f) present the measurements in the upwind buses and in the downwind buses under scenario 5, respectively.

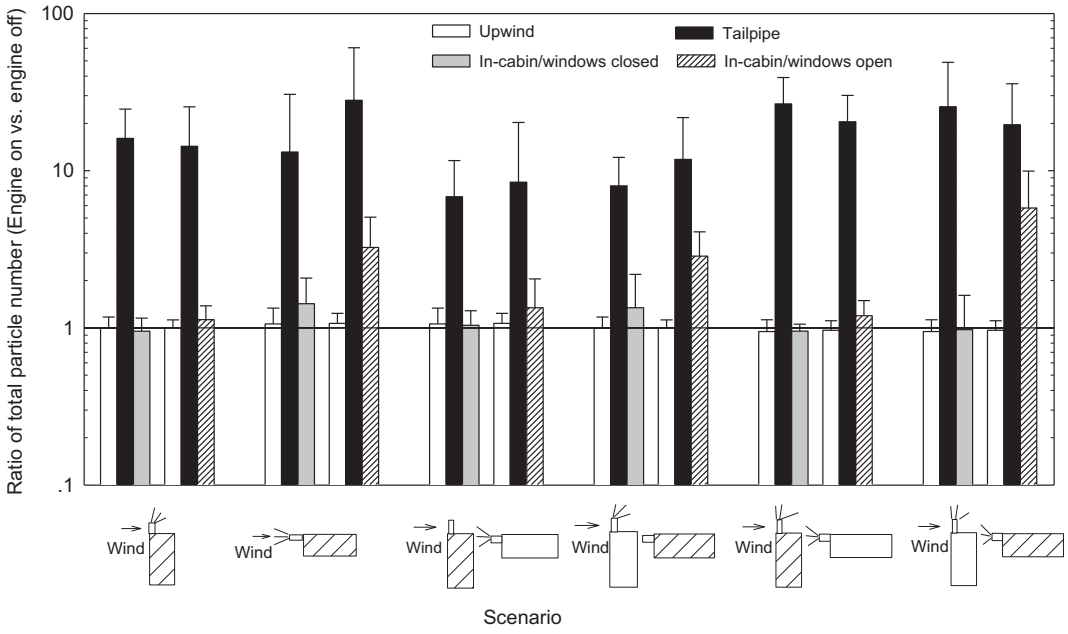

Fig. 3. Ratios of particle number concentration between engine on and engine off conditions under different scenarios. Shaded boxes indicate the buses in which the measurements were shown. Rays indicate the buses of which the engines were turned on. Error bars indicate one standard deviation.

between 1.0 and 1.4, smaller than those measured for open windows, which ranged from 1.2 to 5.8. The greatest ratio, 5.8, was found for Scenario 5 in the downwind bus with open windows.

The change of in-cabin particle number concentration due to idling was not uniform across the size range measured by the SMPS. Fig. 4 shows some selected time series of size-segregated particle number concentration inside bus cabins where significant increase of particle levels was observed after turning on the engines (Fig. 2 (b), (d), and (f) under window open condition). After turning on the engines, the greatest increase occurred in the size range of 10–30 nm. The concentrations of particles in the size range of 40–100 nm also increased, but with much less magnitude. The concentrations of the particles with diameters larger than 100 nm stayed the same. Since most of particles emitted by diesel engines were in nuclei mode with diameters less than 30 nm (Kittelson, 1998), the highest increase of in-cabin UFPs in this size range was expected.

Since the penetration of particles differed greatly by particle size, we used longitudinal regression to analyze particle number concentrations for each particle size bin. Fig. 5 shows the results of longitudinal regression for the particle size distributions inside school bus cabins under different scenarios. Lines represent the mean, and shaded regions indicate 95% confidence interval. Size distribution for the engine off condition is based on data collected when the engines were off over all simulated scenarios. Size distributions for engine on condition were the prediction of in-cabin particle number concentrations after the engines have been running for 15 min. Under the engine off condition, in-cabin UFP counts had a primary mode of 20 nm and a secondary mode of 60 nm. With perpendicular wind, as shown in Fig. 5(a), the in-cabin UFP size distributions did not change due to engine operation. With parallel wind in Fig. 5(b), turning on the engines did not change the modes, but significantly increased the number concentrations of particles with diameters from 10 to 30 nm. The average particle number concentration of the primary mode, 20 nm particle, increased by 110% with windows closed and by 170% with windows open. When the emissions come from a school bus idling nearby, as shown in Fig. 5 (c) and (d), only the downwind buses are affected significantly by tailpipe emissions. Emissions from the upwind buses increase the mean concentrations of the primary mode inside the downwind buses by 50% with windows closed and by 130% with windows open, comparable to the increase in Fig. 5(b). When two buses were idling together, Fig. 5 (e) and (f) show only the downwind buses have a significant increase of in-cabin UFPs. The number concentrations of the primary mode increase by over 500% with windows open, much higher than those in Fig. 5 (b) and (d).

3.2. $PM_{2.5}$ in school buses

Similar to Fig. 2, Fig. 6 summarizes $PM_{2.5}$ mass concentrations for upwind air, in-cabin air, and air close to the tailpipe. Compared with the upwind air, the average $PM_{2.5}$ mass concentrations in the cabins were lower by 3.0–5.8 μg m^{-3} when the windows were closed and by 0.5–4.0 μg m^{-3} when the windows were open. Except for downwind buses with open windows in Fig. 6(f), of which the average $PM_{2.5}$ increased from 10.8 to 13.1 μg m^{-3}, turning on the engines did not change in-cabin $PM_{2.5}$ mass concentrations. The results of longitudinal analysis described in Section 2.5 found no statistically significant difference on in-cabin $PM_{2.5}$ between engine off and engine on conditions for all scenarios. Hence, in-cabin $PM_{2.5}$ mass concentration, different from UFP number concentration, was not strongly affected by local tailpipe emissions. Similarly, Richmond-Bryant et al. (2009) found the $PM_{2.5}$ mass concentration on the street canyon near a cluster of schools was insensitive to diesel vehicles idling nearby. When assessing the impact of tailpipe emissions on particles in school buses, particle number concentration is a more appropriate index than $PM_{2.5}$.

Previous studies have found that in-cabin $PM_{2.5}$ was dominated by the emissions from the crankcase (Hill et al., 2005; Ireson et al., 2011; Liu et al., 2010). Crankcase contributions were not observed in this study. The discrepancy might be explained by bus age. Older school buses have been observed with higher crankcase $PM_{2.5}$

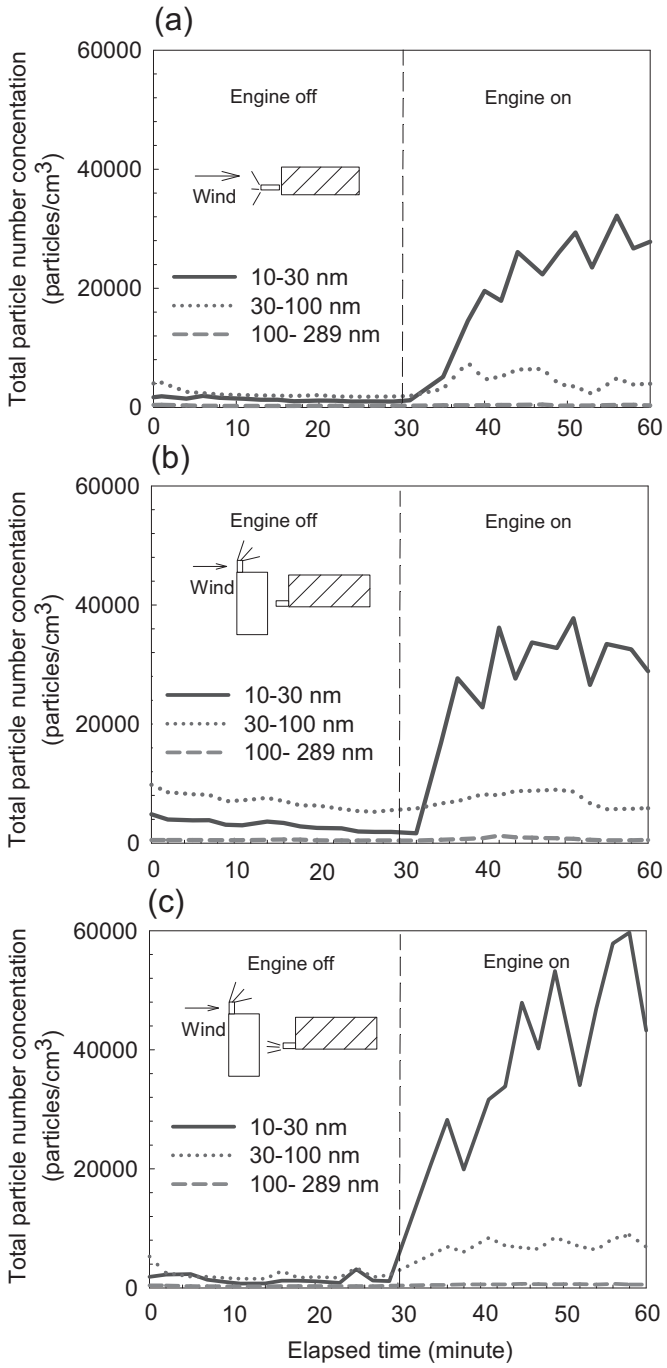

Fig. 4. Selected time series of in-cabin particle number concentrations of different size ranges under the scenarios with significant increase on total particle number concentration. Shaded boxes indicate the buses in which the measurements were shown. Rays indicate the buses of which the engines were turned on.

emission rates than newer buses (Adar et al., 2008; Liu et al., 2010; Zielinska et al., 2008). Newer buses usually had fewer cracks or leaks in the crankcases and in the bus floors. In addition newer buses had engines under the front hoods, but the older buses had their engines under the cabin floor, increasing the chance of contamination from crankcase emissions. In 2000, U.S. EPA announced the new PM emission standard for new heavy-duty engines and required the control of crankcase emissions (U.S.EPA, 2001). Manufacturers of school buses may therefore have adopted new designs to control crankcase emissions, such as sealed crankcase oil systems or routing of crankcase emissions to the engine air intake system. In this study the majority of tested school buses were of 2005 model year with engines under the front hoods, so $PM_{2.5}$ from crankcase emissions was expected to be less important.

3.3. Factors affecting particle penetration

Total particle number concentrations measured close to tailpipes were consistently high for all simulated scenarios, but in-cabin total particle number concentrations varied over the different scenarios. We used a longitudinal model to estimate the effects of emission source, wind direction, window position, and their interactions on in-cabin particle number concentrations of different sizes. Emission source made no significant difference on particle counts of any size, regardless of wind direction or window position. The implication is that it is insufficient to protect children in a school bus by merely shutting down its own engines. Any school bus idling nearby may introduce similar levels of diesel particles to the bus own emissions.

Wind direction and window position had important impact on in-cabin particle number concentration. Fig. 7 presents *p*-values for the effect of wind, window, and their interaction on in-cabin particle number concentration of each size. For particles in the size range of 10–30 nm, *p*-values were usually less than 0.05, indicating wind direction played a significant role in introducing nuclei mode particles freshly emitted by tailpipes into buses' cabins, regardless of window position or the emission source. No significant effect was found for window position itself, but the interaction of wind and window was significant. The effect of window position depends on wind direction. Specifically only when the wind blew from the tailpipe to the hood, did open windows cause higher particle concentrations. Fig. 7 also confirms the insensitivity of in-cabin $PM_{2.5}$ mass concentration, which was dominated by large particles, to the tailpipe emissions from idling school buses shown in Fig. 6.

Idling school buses greatly increase particle number concentrations close to the tailpipe and in-cabin UFPs under some scenarios, therefore anti-idling rules would reduce school children's exposure to diesel particles substantially. However, there might be some circumstances that idling could not be avoided. In this case, lower exposure might be achieved by laying out school buses at bus transfer stations and parking lots according to local meteorological condition so that for the majority of operation periods, no school bus is parked downwind of tailpipe emissions from itself or other buses. If good bus parking arrangements are not feasible, school bus windows should be closed while idling.

3.4. Air exchange rate and deposition rate

After penetrating into bus cabins, particles may be removed by several mechanisms, such as outdoor air exchange or surface deposition. Table 2 summarized air exchange rates and deposition rates for the nine tested school buses. With closed windows, air exchange rates in the stationary buses varied between 0.6 h^{-1} and 5.6 h^{-1}. When windows were open, the air exchange rates were greater, ranging from 11.1 h^{-1}–34.4 h^{-1}. These results were comparable to air exchange rates in school buses reported by previous studies (Sabin et al., 2005).

Table 2 also presents the deposition rates for total particle number concentration inside bus cabins, which varied between 1.5 and 5.0 h^{-1} under natural convection condition among the tested

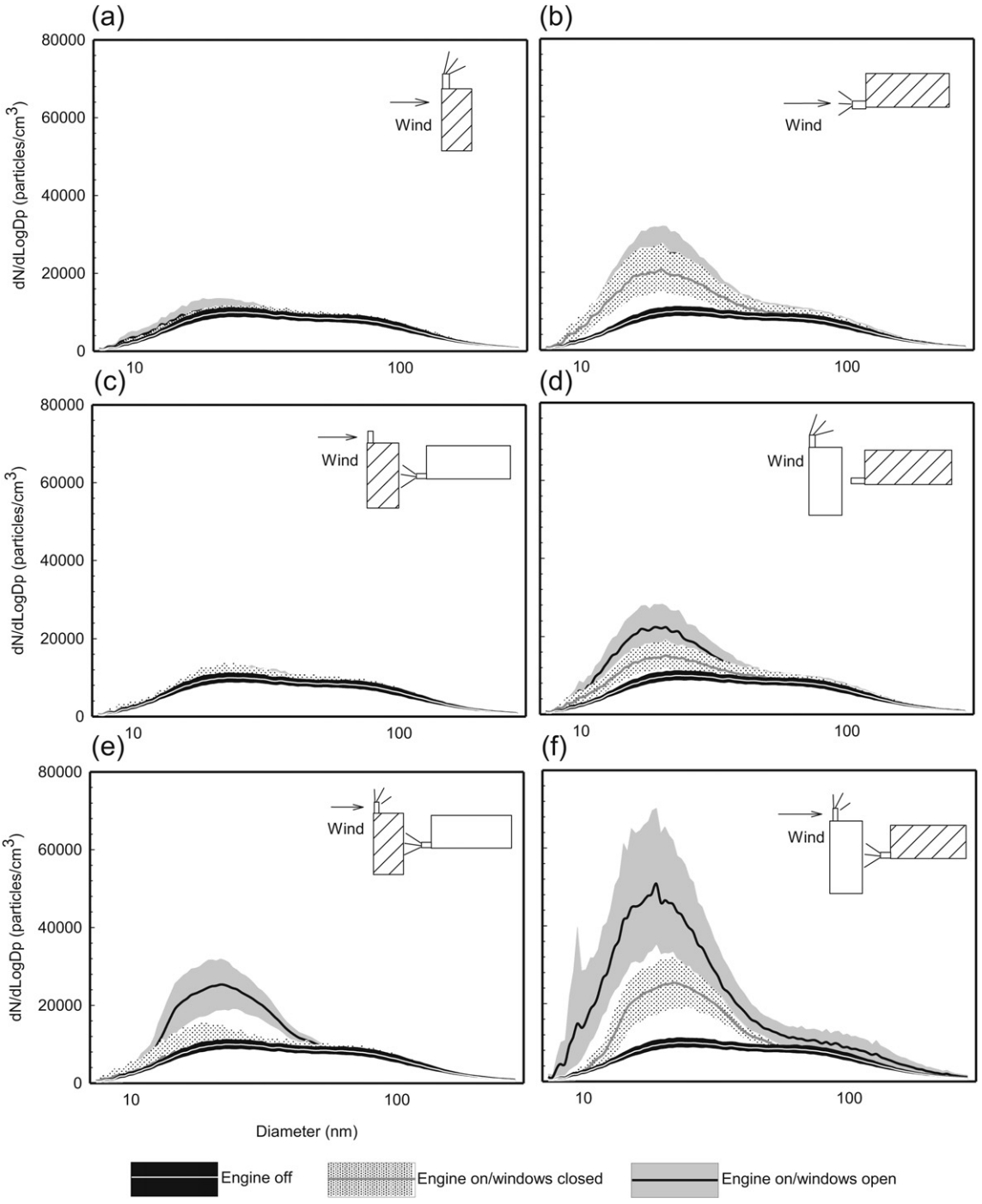

Fig. 5. Simulated size distributions of UFPs inside school buses under different scenarios. Solid lines indicate the means and shaded regions indicate 95% confidence intervals.

school buses. Fig. 8 presents the size-resolved deposition rates inside school buses compared with the measurements in passenger cars and residential indoor environments from previous studies. Similar to indoor and in-cabin environments, the size-resolved deposition rate inside school bus cabins was a strong function of particle sizes. The average deposition rate of 10 nm particles was 8.0 h^{-1}, 5.5 times higher than 100 nm particles due to greater diffusion for smaller particles. Across the measured size range, the deposition rates inside school buses were about 1/5–1/3 of that inside passenger cars (Gong et al., 2009), and 1.6–2.7 times higher than that in a 26 m^3 residential apartment (Zhu et al., 2005). Gong et al. (2009) found higher surface area to volume (S/V) ratios favored higher UFP deposition rates. For the tested school buses, although the in-cabin volume and the interior surface areas varied widely, the S/V ratios of these buses were fairly consistent, ranging from 2.5 to 2.9. These S/V ratios were smaller than the 4.0–8.1 for passenger cars (Gong et al., 2009) but larger than around 2.0 for the residential apartment (Zhu et al., 2005), which may explain the difference in UFP deposition rates among these three environments.

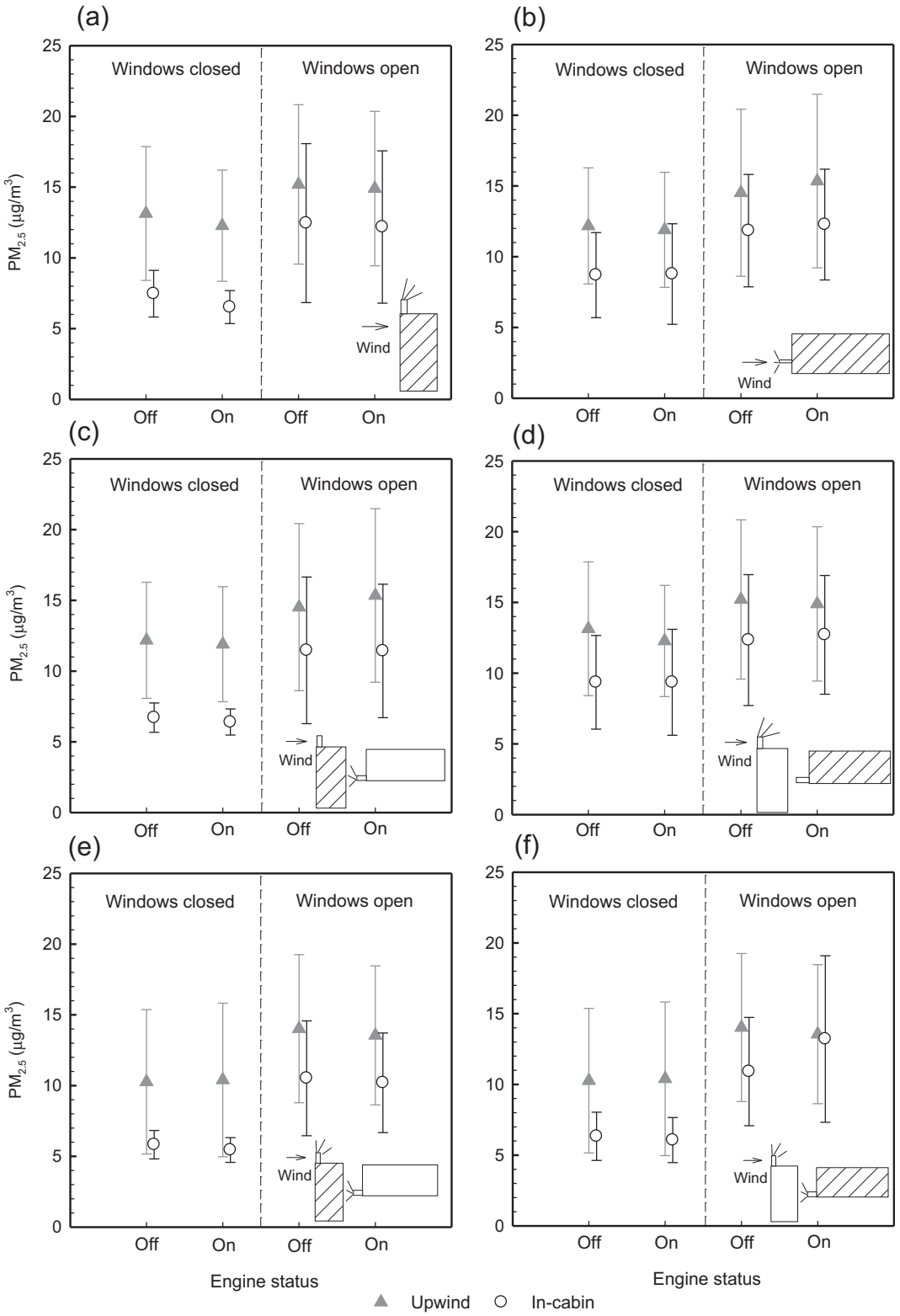

Fig. 6. $PM_{2.5}$ mass concentrations in upwind air, in-cabin air, and air close to the tailpipes under different scenarios with different window positions. Shaded boxes indicate the buses in which the measurements come from. Rays indicate the buses for which the engines were turned on. Error bars indicate one standard deviation. Figures (a) – (d) present scenarios 1 – 4 and (e) – (f) present the measurements in the upwind buses and in the downwind buses under scenario 5, respectively.

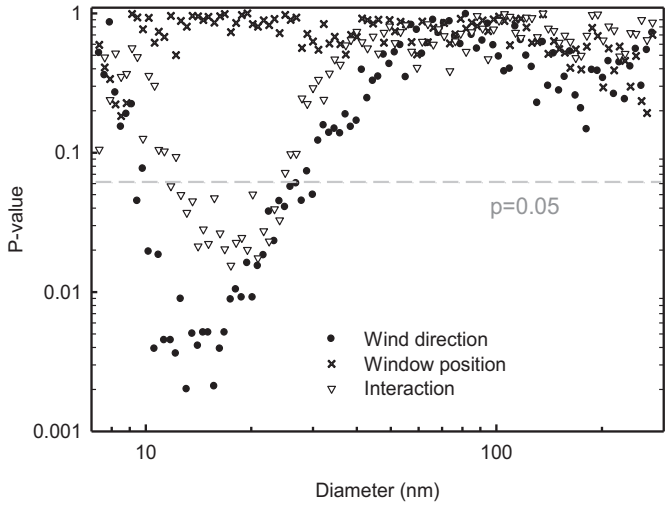

Fig. 7. *P*-values for the effect of wind, window, and their interaction. Horizontal line drawn at $p = 0.05$.

Table 2
Air exchange rate and particle deposition rate inside school buses.

Bus ID	Air exchange rate (h^{-1})		Deposition rate[a] (h^{-1})
	Windows closed	Windows open	
1	4.6	30.1	2.3
2	0.6	34.0	3.7
3	1.7	15.2	2.8
4	3.9	22.2	4.2
5	1.7	34.4	4.5
6	1.1	11.1	1.5
7	1.9	27.6	3.3
8	3.5	14.7	5.0
9	5.6	30.8	3.9

[a] Deposition rates were calculated based on total particle number concentration.

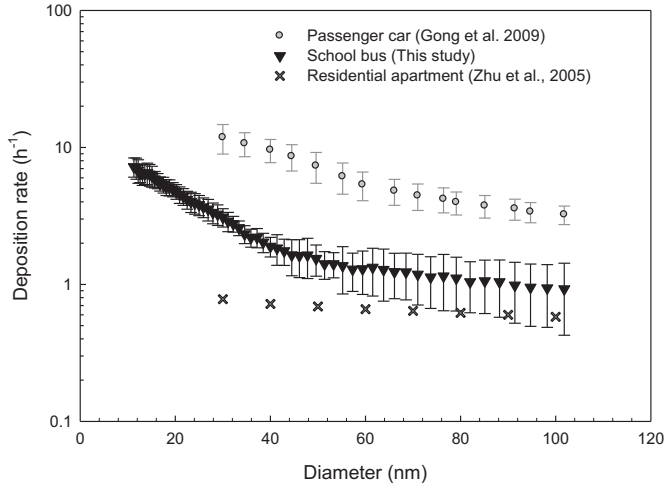

Fig. 8. Comparison of UFP deposition rates inside school buses vs. passenger cars and residential houses.

4. Conclusions

Idling school buses significantly increased the particle number concentration for air close to tailpipes by a factor of up to 26 under all scenarios simulated in this study. After turning on the engines, the potential exposure to diesel particles for children present near school buses increased sharply from the background level to as high as 3.2×10^5 particles/cm^3. Diesel emissions from idling school buses also have important impact on in-cabin particle number concentrations under certain conditions. Wind direction played a significant role for the penetration of tailpipe-emitted particles into bus cabins. The effect of window positions depended on wind direction. When wind carried diesel emissions from tailpipe toward hood, total particle number concentration inside school buses with open windows increased significantly by a factor of up to 5.8, with the greatest increase occurring in the size range of 10–30 nm. Wind speed may also play an important role for the penetration of diesel emissions from tailpipe into bus cabins. Because wind speed was relatively stable in the study area and is difficult to manipulate, a physical-based numerical model may be an alternative method to better understand the role of wind speed in future studies.

No significant change of in-cabin $PM_{2.5}$ mass concentration was observed with or without tailpipe emissions, regardless of wind direction and window position, indicating that $PM_{2.5}$ may be insufficient for assessing the exposures to primary diesel emissions from idling school buses.

The air exchange rates in the stationary school buses were 0.6–5.6 h^{-1} when the windows were closed, and 11.1–34.4 h^{-1} when the windows were open. The deposition rates for total particle number concentration varied between 1.5 and 5.0 h^{-1} across the tested school buses under natural convection conditions, which were lower than those of passenger cars but higher than those of indoor environments.

Acknowledgments

The study is supported by the Health Effects Institute's Walter A. Rosenblith New Investigator Award under contract #4764-FRA06-3107-5 and National Science Foundation's CAREER Award under contract # 32525-A6010 AI. Authors appreciate the cooperation of Tumbleweed Transportation, CA for providing school buses. We acknowledge Bin Xu for his assistance in the field.

Appendix A. Supplementary data

Supplementary data related to this article can be found at http://dx.doi.org/10.1016/j.atmosenv.2012.12.015.

References

Adar, S.D., Davey, M., Sullivan, J.R., Compher, M., Szpiro, A., Liu, L.J.S., 2008. Predicting airborne particle levels aboard Washington State school buses. Atmospheric Environment 42, 7590–7599.
Alessandrini, F., Schulz, H., Takenaka, S., Lentner, B., Karg, E., Behrendt, H., Jakob, T., 2006. Effects of ultrafine carbon particle inhalation on allergic inflammation of the lung. Journal of Allergy and Clinical Immunology 117, 824–830.
Behrentz, E., Fitz, D.R., Pankratz, D.V., Sabin, L.D., Colome, S.D., Fruin, S.A., Winer, A.M., 2004. Measuring self-pollution in school buses using a tracer gas technique. Atmospheric Environment 38, 3735–3746.
Behrentz, E., Sabin, L.D., Winer, A.M., Fitz, D.R., Pankratz, D.V., Colome, S.D., Fruin, S.A., 2005. Relative importance of school bus-related microenvironments to children's pollutant exposure. Journal of the Air & Waste Management Association 55, 1418–1430.
Bennett, W.D., Zeman, K.L., 1998. Deposition of fine particles in children spontaneously breathing at rest. Inhalation Toxicology 10, 831–842.
Delfino, R.J., Sioutas, C., Malik, S., 2005. Potential role of ultrafine particles in associations between airborne particle mass and cardiovascular health. Environmental Health Perspectives 113, 934–946.
Ferin, J., Oberdorster, G., Penney, D.P., Soderholm, S.C., Gelein, R., Piper, H.C., 1990. Increased pulmonary toxicity of ultrafine particles? I. particle clearance, translocation, morphology. Journal of Aerosol Science 21, 384–387.
Frampton, M.W., Stewart, J.C., Oberdorster, G., Morrow, P.E., Chalupa, D., Pietropaoli, A.P., Frasier, L.M., Speers, D.M., Cox, C., Huang, L.S., Utell, M.J., 2006. Inhalation of ultrafine particles alters blood leukocyte expression of adhesion molecules in humans. Environmental Health Perspectives 114, 51–58.

Gong, L., Xu, B., Zhu, Y., 2009. Ultrafine particles deposition inside passenger vehicles. Aerosol Science and Technology 43, 544–553.
Hill, L.B., Zimmerman, N.B., Gooch, J., 2005. A Multi-city Investigation of the Effectiveness of Retrofit Emissions Controls in Reducing Exposures to Particulate Matter in School Buses. Clean Air Task Force, Boston, MA.
Hochstetler, H.A., Yermakov, M., Reponen, T., Ryan, P.H., Grinshpun, S.A., 2010. Aerosol particles generated by diesel-powered school buses at urban schools as a source of children's exposure. Atmospheric Environment 45, 1444–1453.
Ireson, R.G., Easter, M.D., Lakin, M.L., Ondov, J.M., Clark, N.N., Wright, D.B., 2004. Estimation of diesel particulate matter concentrations in a school bus using a fuel-based tracer - sensitive and specific method for quantifying vehicle contributions. Energy and Environmental Concerns, 21–28.
Ireson, R.G., Ondov, J.M., Zielinska, B., Weaver, C.S., Easter, M.D., Lawson, D.R., Hesterberg, T.W., Davey, M.E., Liu, L.-J.S., 2011. Measuring in-cabin school bus tailpipe and crankcase PM2.5: a new dual tracer method. Journal of the Air & Waste Management Association 61, 494–503.
Jayaratne, E.R., Ristovski, Z.D., Meyer, N., Morawska, L., 2009. Particle and gaseous emissions from compressed natural gas and ultra low sulphur diesel-fuelled buses at four steady engine loads. Science of the Total Environment 407, 2845–2852.
Kittelson, D.B., 1998. Engines and nanoparticles: a review. Journal of Aerosol Science 29, 575–588.
Liu, L.J.S., Phuleria, H.C., Webber, W., Davey, M., Lawson, D.R., Ireson, R.G., Zielinska, B., Ondov, J.M., Weaver, C.S., Lapin, C.A., Easter, M., Hesterberg, T.W., Larson, T., 2010. Quantification of self pollution from two diesel school buses using three independent methods. Atmospheric Environment 44, 3422–3431.
Marshall, J.D., Behrentz, E., 2005. Vehicle self-pollution intake fraction: children's exposure to school bus emissions. Environmental Science & Technology 39, 2559–2563.
Oberdorster, G., Sharp, Z., Atudorei, V., Elder, A., Gelein, R., Kreyling, W., Cox, C., 2004. Translocation of inhaled ultrafine particles to the brain. Inhalation Toxicology 16, 437–445.
Ott, W., Klepeis, N., Switzer, P., 2008. Air change rates of motor vehicles and in-vehicle pollutant concentrations from secondhand smoke. Journal of Exposure Science and Environmental Epidemiology 18, 312–325.
Richmond-Bryant, J., Bukiewicz, L., Kalin, R., Galarraga, C., Mirer, F., 2011. A multi-site analysis of the association between black carbon concentrations and vehicular idling, traffic, background pollution, and meteorology during school dismissals. Science of the Total Environment 409, 2085–2093.
Richmond-Bryant, J., Saganich, C., Bukiewicz, L., Kalin, R., 2009. Associations of PM2.5 and black carbon concentrations with traffic, idling, background pollution, and meteorology during school dismissals. Science of the Total Environment 407, 3357–3364.
Sabin, L.D., Behrentz, E., Winer, A.M., Jeong, S., Fitz, D.R., Pankratz, D.V., Colome, S.D., Fruin, S.A., 2005. Characterizing the range of children's air pollutant exposure during school bus commutes. Journal of Exposure Analysis and Environmental Epidemiology 15, 377–387.
Samet, J.M., Rappold, A., Graff, D., Cascio, W.E., Berntsen, J.H., Huang, Y.C.T., Herbst, M., Bassett, M., Montilla, T., Hazucha, M.J., Bromberg, P.A., Devlin, R.B., 2009. Concentrated ambient ultrafine particle exposure induces cardiac changes in young healthy volunteers. American Journal of Respiratory and Critical Care Medicine 179, 1034–1042.
U.S.EPA, 2001. Control of Air Pollution from New Motor Vehicles: Heavy Duty Engine and Vehicle Standards and Highway Diesel Fuel Sulfur Control Requirements, Final Rule. 66 FR 5002. the United States Environmental Protection Agency.
U.S.EPA, 2002. Health Assessment Document for Diesel Engine Exhaust. EPA/600/8-90/057F. the National Technical Information Service, Springfield, VA.
U.S.EPA, 2012. Clean School Bus USA. Available from: http://www.epa.gov/cleanschoolbus/basicinfo.htm (accessed 04.01.12.).
Weiss, R.E., 2005. Modeling Longitudinal Data. Springer-Verlag, New York.
Zhang, Q., Zhu, Y., 2011. Performance of school bus retrofit systems: ultrafine particles and other vehicular pollutants. Environmental Science & Technology 45, 6475–6482.
Zhang, Q.F., Zhu, Y.F., 2010. Measurements of ultrafine particles and other vehicular pollutants inside school buses in South Texas. Atmospheric Environment 44, 253–261.
Zhu, Y.F., Hinds, W.C., Krudysz, M., Kuhn, T., Froines, J., Sioutas, C., 2005. Penetration of freeway ultrafine particles into indoor environments. Journal of Aerosol Science 36, 303–322.
Zielinska, B., Campbell, D., Lawson, D.R., Ireson, R.G., Weaver, C.S., Hesterberg, T.W., Larson, T., Davey, M., Liu, L.J.S., 2008. Detailed characterization and profiles of crankcase and diesel particulate matter exhaust emissions using speciated organics. Environmental Science & Technology 42, 5661–5666.